Age Hardening

The reason for the interest in alloy systems that show transition phase precipitation is that great improvements in the mechanical properties of these alloys can be achieved by suitable solution treatment and ageing operations. This is illustrated for various Al–Cu alloys in Fig. The alloys were solution treated in the single-phase α region of the phase diagram, quenched to room temperature and aged at either 130°C (Fig-a) or 190°C (Fig-b). The curves show how the hardness of the specimens varies as a function of time and the range of time over which GP zones, θ'' and θ' appear in the microstructure. Immediately after quenching the main resistance to dislocation movement is solid solution hardening. The specimen is relatively easily deformed at this stage and the hardness is low. As GP zones form the hardness increases due to the extra stress required to force dislocations through the coherent zones.

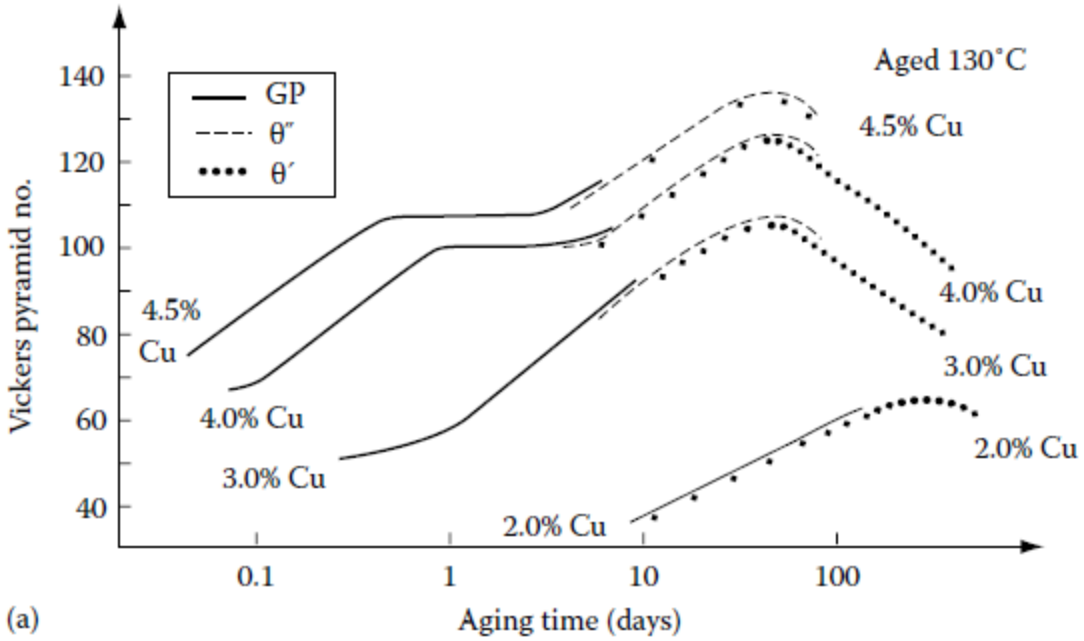
Aged 130°C
GP
θ″
θ′
4.5% Cu
4.0% Cu
3.0% Cu
2.0% Cu
4.5% Cu
4.0% Cu
3.0% Cu
2.0% Cu
Vickers pyramid no.
140
120
100
80
60
40
0.1
1
10
100
Aging time (days)

(a)

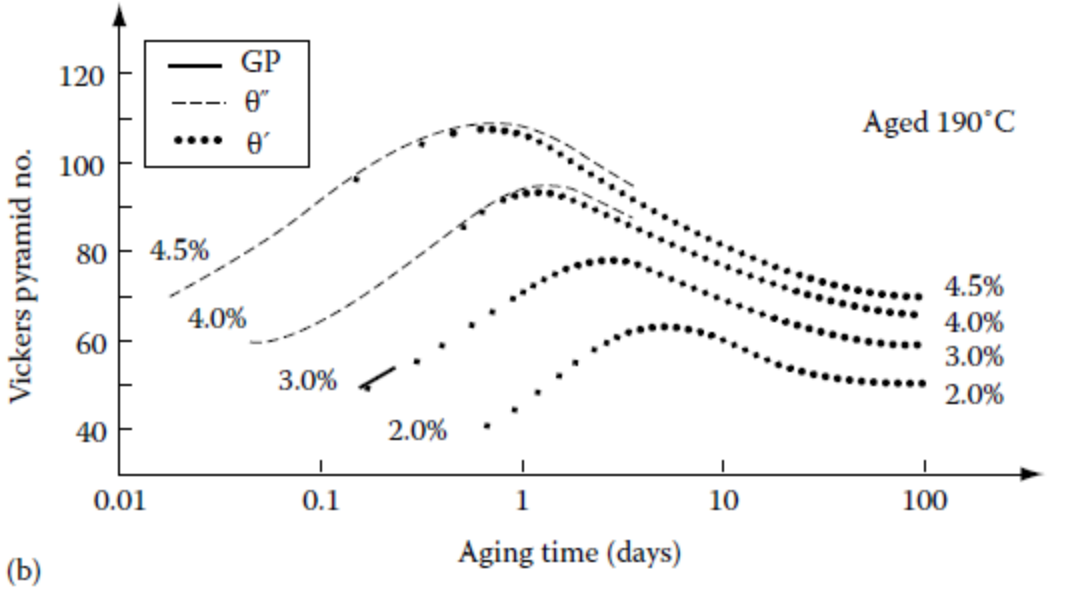
Aged 190°C
GP
θ″
θ′
4.5%
4.0%
3.0%
2.0%
4.5%
4.0%
3.0%
2.0%
Vickers pyramid no.
120
100
80
60
40
0.01
0.1
1
10
100
Aging time (days)

(b)

The hardness continues to increase with the formation of the coherent θ'' precipitates because now the dislocations must also be forced through the highly strained matrix that results from the misfit perpendicular to the θ'' plates. Eventually, with the formation of θ' the spacing between the precipitates becomes so large that the dislocations are able to bow between the precipitates and the hardness begins to decrease. Maximum hardness is associated with a combination of θ'' and θ'. Further ageing increases the distance between the precipitates making dislocation bowing easier and the hardness decreases. Specimens aged beyond peak hardness are referred to as *overaged.*

- If Al–4.5 wt% Cu is aged at 190°C,GP zones are unstable and the first precipitate to form is θ'.

- It can be seen that at 130°C peak hardness in the Al-4.5 wt% Cu alloy is not reached for several tens of days. The temperatures that can be used in the heat treatment of commercial alloys are limited by economic considerations to those which produce the desired properties within a reasonable period of time, usually up to ~24 h.

Spinodal Decomposition

There are certain transformations where there is no barrier to nucleation. One of these is the spinodal mode of transformation. Consider a phase diagram with a miscibility gap as shown in Fig-a. If an alloy with composition X_0 is solution treated at a high temperature T_1 and then quenched to a lower temperature T_2 the composition will initially be the same everywhere and its free energy will be G_0 on the G curve in Fig-b.

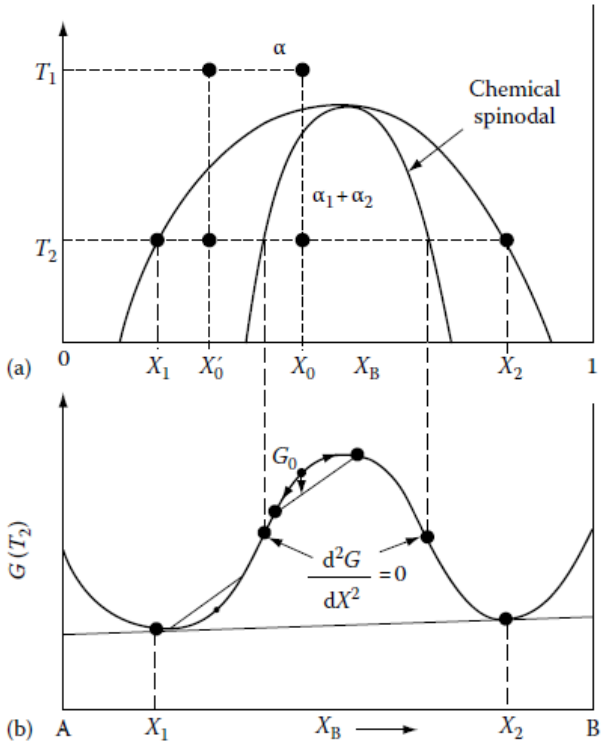

Alloys between the spinodai points are unstable and can decompose into two coherent phases α_1 and α_2 without overcoming an activation energy barrier. Alloys between the coherent miscibility gaps and the spinodai are metastable and can decompose only after nucleation of the other phase.

However, the alloy will be immediately *unstable* because small fluctuations in composition that produce A-rich and B-rich regions will cause the total free energy to decrease. Therefore 'up-hill' diffusion takes place as shown in Fig until the equilibrium compositions X_1 and X_2 are reached.

The above process can occur for any alloy composition where the free energy curve has a negative curvature, i.e.

$$\frac{d^2G}{dX^2} < 0$$

Therefore the alloy must lie between the two points of inflection on the free energy curve. The locations of the points on the phase diagram, Fig-a, is known as the chemical spinodai.

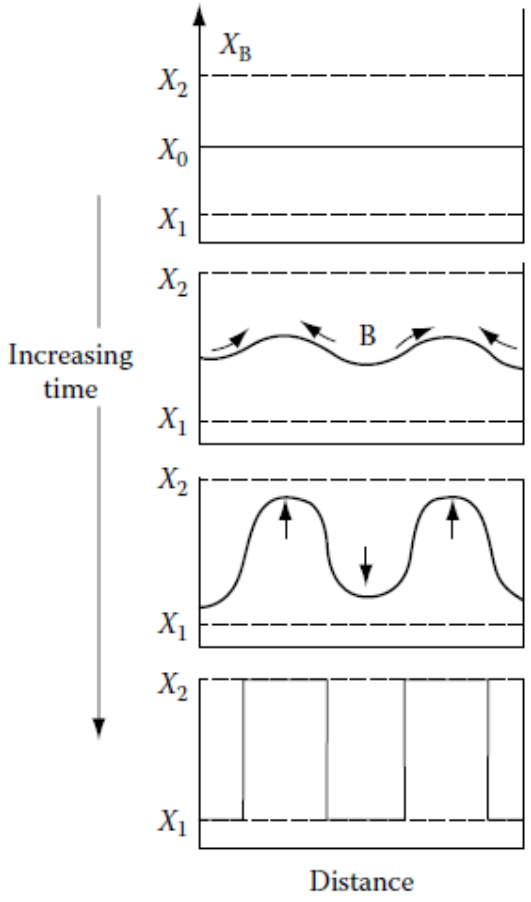

If the alloy lies outside the spinodai, small variations in composition lead to an increase in free energy and the alloy is therefore *metastable.* The free energy of the system can only be decreased in this case if nuclei are formed with a composition very different from the matrix. Therefore, outside the spinodai the transformation must proceed by a process of nucleation and growth. Normal down-hill diffusion occurs in this case as shown in Fig.

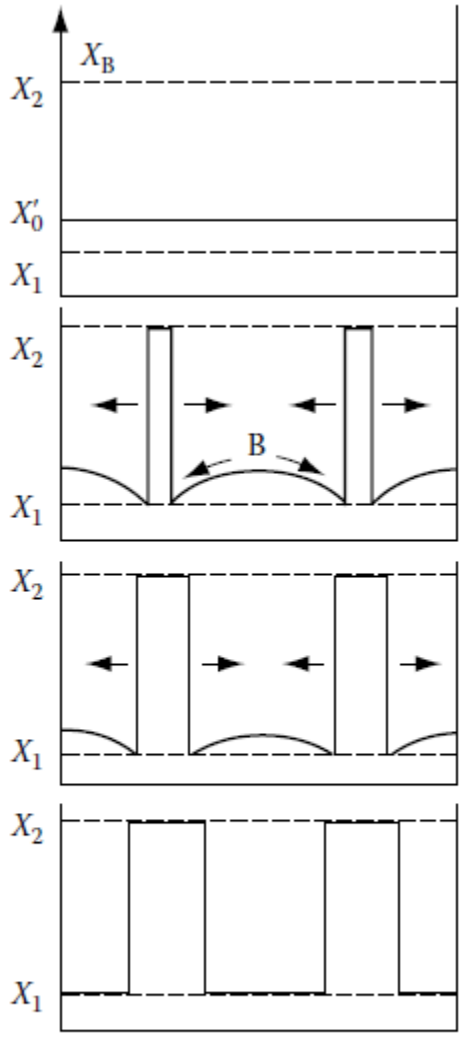

Schematic composition profiles at increasing times in an alloy outside the spinodal points

Particle Coarsening

The microstructure of a two-phase alloy is always unstable if the total interfacial free energy is not a minimum. Therefore a high density of small precipitates will tend to *coarsen* into a lower density of larger particles with a smaller total interfacial area. However, such coarsening often produces an undesirable degradation of properties such as a loss of strength or the disappearance of grain-boundary pinning effects. As with grain growth, the rate of coarsening increases with temperature and is of particular concern in the design of materials for high temperature applications.

In any precipitation-hardened specimen there will be a range of particle sizes due to differences in the time of nucleation and rate of growth. Consider two adjacent spherical precipitates with different diameters as shown in Figure.

The solute concentration in the matrix adjacent to a particle will increase as the radius of curvature decreases, Fig-b.

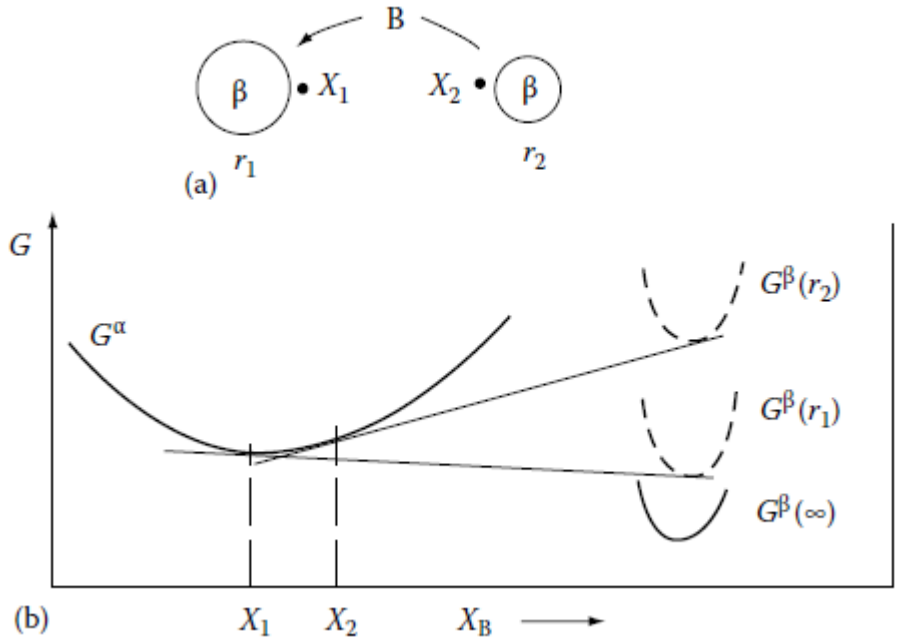

Therefore there will be concentration gradients in the matrix which will cause solute to diffuse in the direction of the largest particles away from the smallest, so that the small particles shrink and disappear while large particles grow.

The overall result is that the total number of particles decreases and the mean radius ($\bar{r}$) increases with time. By assuming volume diffusion is the rate controlling factor it has been shown relationship should be obeyed:

$$(\bar{r})^3 - r_0^3 = kt \qquad \text{where} \qquad k \alpha D\gamma X_e$$

r_0 is the mean radius at time $t = 0$, D is the diffusion coefficient, γ is the interfacial energy and X_e is the equilibrium solubility of very large particles.

Since D and X_e increase exponentially with temperature, the rate of coarsening will increase rapidly with increasing temperature

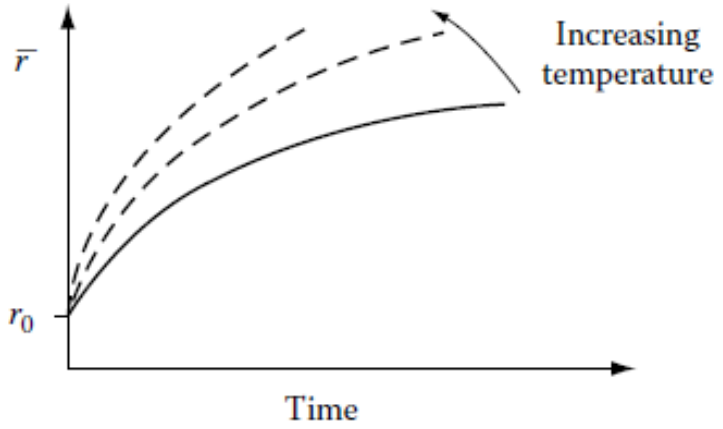

In practice the rate at which particles coarsen may not follow a linear r^3-t relationship. Deviations from this relationship can be caused by diffusion short-circuits such as dislocations, or grain boundaries. Also the coarsening rate may be interface controlled. Nevertheless, apart from the case of interface control, the rate of coarsening should depend on the product $D\gamma X_e$, Therefore high temperature alloys whose strength depends on a fine precipitate dispersion must have a low value for at least one of γ, X_e or D. Let us consider examples of each of these.

Low γ

The heat-resistant *Nimonic* alloys based on Ni–Cr with additions of Al and Ti obtain their high strength from a fine dispersion of the ordered fcc phase $Ni_3(TiAl)$ (γ') which precipitates in the fcc Ni-rich matrix. The Ni/γ' interfaces are fully coherent and the interfacial energy is exceptionally low ($\sim$10–30 mJ m^{-2}) which enables the alloys to maintain a fine structure at high temperature. The misfit between the precipitates and matrix varies between zero and about 0.2% depending on composition.

Low X_e

High strength at high temperatures can also be obtained with fine oxide dispersions in a metal matrix. For example W and Ni can be strengthened for high temperature use by fine dispersions of thoria ThO_2. In general, oxides are very insoluble in metals and the stability of these microstructures at high temperatures can be attributed to a low value of X_e in the product $D\gamma X_e$.

Low D

Cementite dispersions in tempered steels coarsen very quickly due to the high diffusivity of interstitial carbon. However, if the steel contains a substitutional alloying element that segregates to the carbide, the rate of coarsening becomes limited by the much slower rate at which substitutional diffusion can occur. If the carbide-forming element is present in high concentrations more stable carbides are formed which have the additional advantage of a lower solubility (X_e). Therefore low-alloy steels used for medium temperature creep resistance often have additions of strong carbide-forming elements.

Cellular Precipitation

Grain-boundary precipitation does not always result in Widmanstatten side-plates or needles. In some cases it can result in a different mode of transformation, known as *cellular precipitation.* The essential feature of this type of transformation is that the boundary moves with the growing tips of the precipitates as shown in Fig. Morphologically the transformation is very similar to the eutectoid reaction. However, in this case the reaction can be written

$$\alpha' \rightarrow \alpha + \beta$$

where α' is the supersaturated matrix, α is the *same phase* but with a lower thermodynamic excess of solute, and β is the equilibrium precipitate.

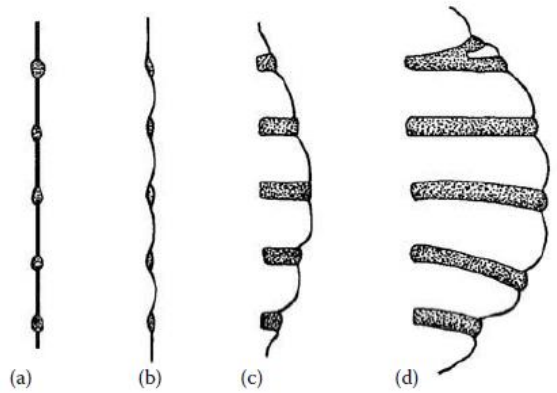

The mechanism whereby grain-boundary nucleation develops into cellular precipitation differs from one alloy to another and is not always fully understood. The reason why cells develop in some alloys and not in others is also unclear.

Figure shows an example of cellular precipitation in a Mg-9 atomic % Al alloy. The β phase in this case is the equilibrium precipitate $Mg_{17}Al_{12}$ indicated in the phase diagram figure.

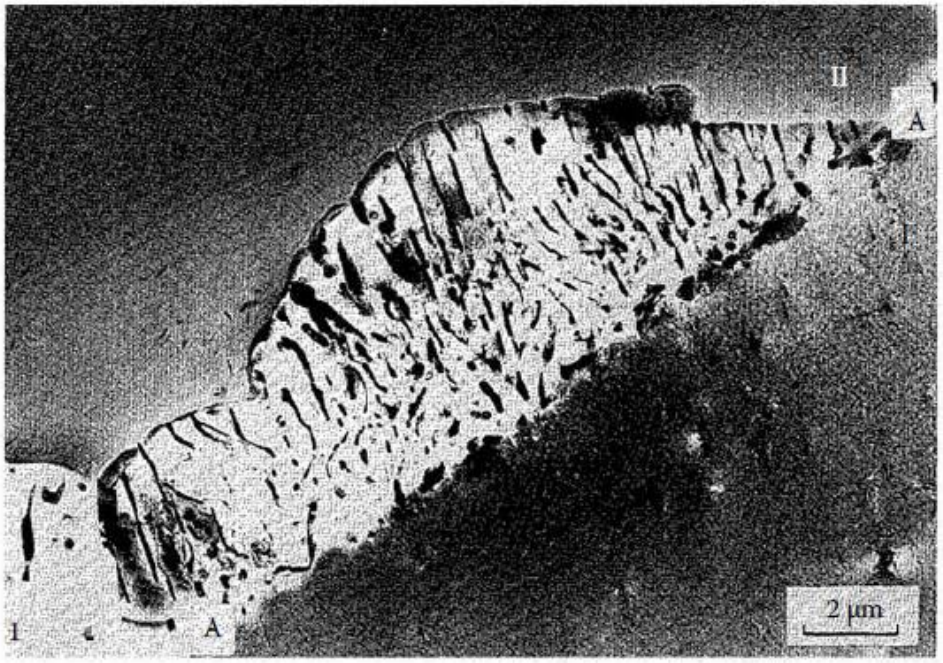

It can be seen in previous Fig. that the $Mg_{17}Al_{12}$ forms as lamellae embedded in a Mg-rich matrix.

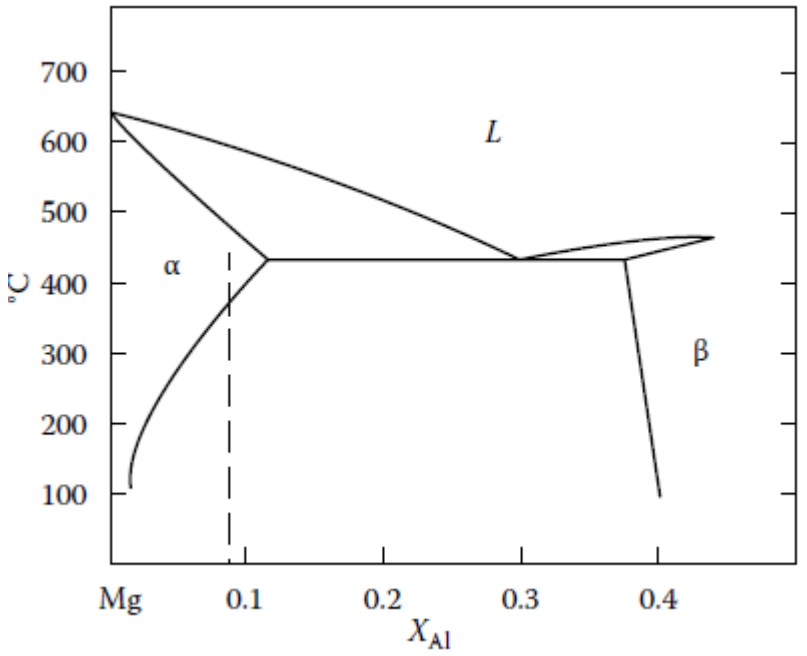

Figure below shows another specimen which has been given a two-stage heat treatment. After solution treating at 410°C the specimen was quenched to a temperature of 220°C for 20 min followed by 90 s at 277°C and finally water quenched. It is apparent that the mean interlamellar spacing is higher at higher ageing temperatures

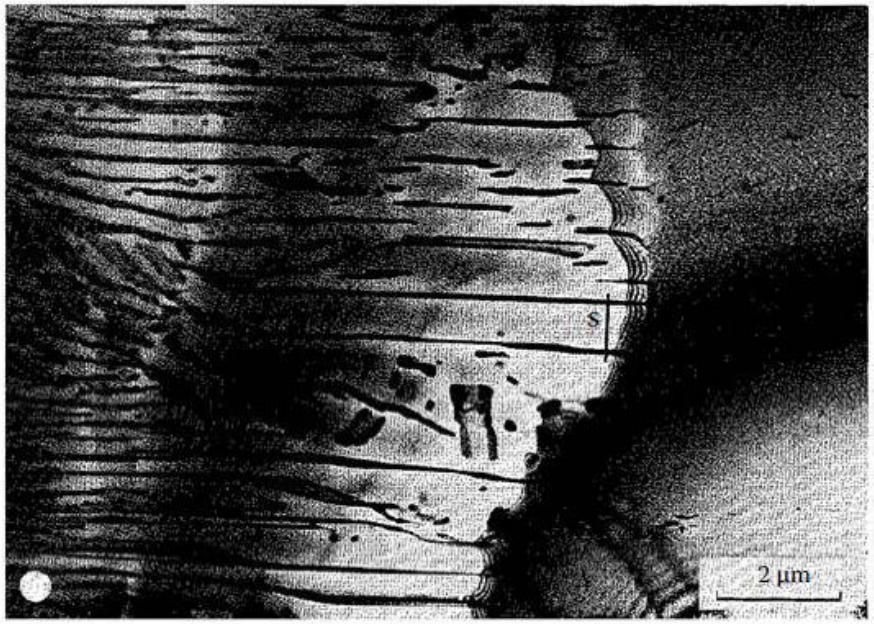

The growth of cellular precipitates requires the partitioning/separating of solute to the tips of the precipitates in contact with the advancing grain boundary. This can occur in one of two ways: either by ***diffusion through the lattice*** ahead of the advancing cell front, or by ***diffusion in the moving boundary***. Partitioning by lattice diffusion would require solute concentration gradients ahead of the cell front while, if the grain boundary is the most effective diffusion route, the matrix composition should remain unchanged right up to the cell front. In the case of the Mg–Al alloy it has been possible to do microanalysis with sufficiently high spatial resolution to resolve these possibilities directly. (The technique used was electron energy loss spectroscopy using plasmon losses) The results of such measurements, Fig-a below, clearly indicate that the matrix composition remains unchanged to within 10 nm of the advancing cell front so that partitioning must be taking place within the boundary itself.

This is to be expected since precipitation is occurring at relatively low temperatures where solute transport tends to become more effective via grain boundaries than through the lattice.

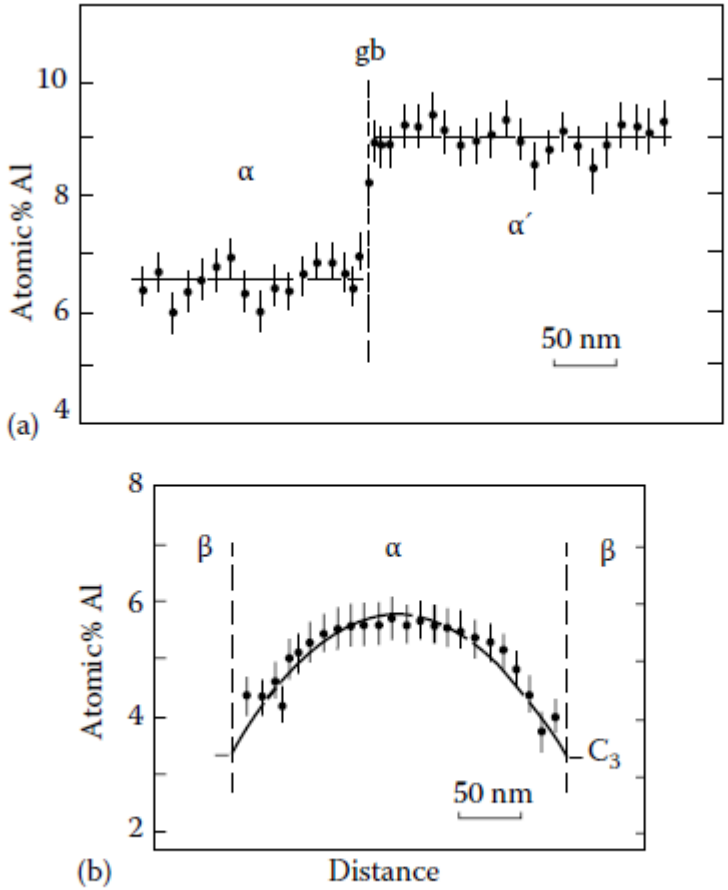

(a) The variation of aluminum concentration across an advancing grain boundary midway between two precipitate lamellae, (b) A similar profile along a line

Cellular precipitation is also known as *discontinuous precipitation* because the composition of the matrix changes discontinuously as the cell front passes. Precipitation that is not cellular is referred to as general or continuous because it occurs generally throughout the matrix on dislocations or grain boundaries, etc. and the matrix composition at a given point decreases continuously with time.

Eutectoid Transformations

The Pearlite Reaction in Fe–C Alloys

When austenite containing about 0.8 wt% C is cooled below the A_1 temperature it becomes simultaneously supersaturated with respect to ferrite and cementite and a eutectoid transformation results, i.e.

$$\gamma \rightarrow \alpha + Fe_3C$$

The manner in which this reaction occurs is very similar to a eutectic transformation where the original phase is a liquid instead of a solid. In the case of Fe–C alloys the resultant microstructure comprises lamellae, or sheets, of cementite embedded in ferrite as shown in Fig.

This is known as pearlite. Both cementite and ferrite form directly in contact with the austenite as shown. Pearlite nodules nucleate on grain boundaries and grow with a roughly constant radial velocity into the surrounding austenite grains. At small undercoolings below $A_{1(\text{eutectoid T})}$) the number of pearlite nodules that nucleate is relatively small, and the nodules can grow as hemispheres or spheres without interfering with each other.

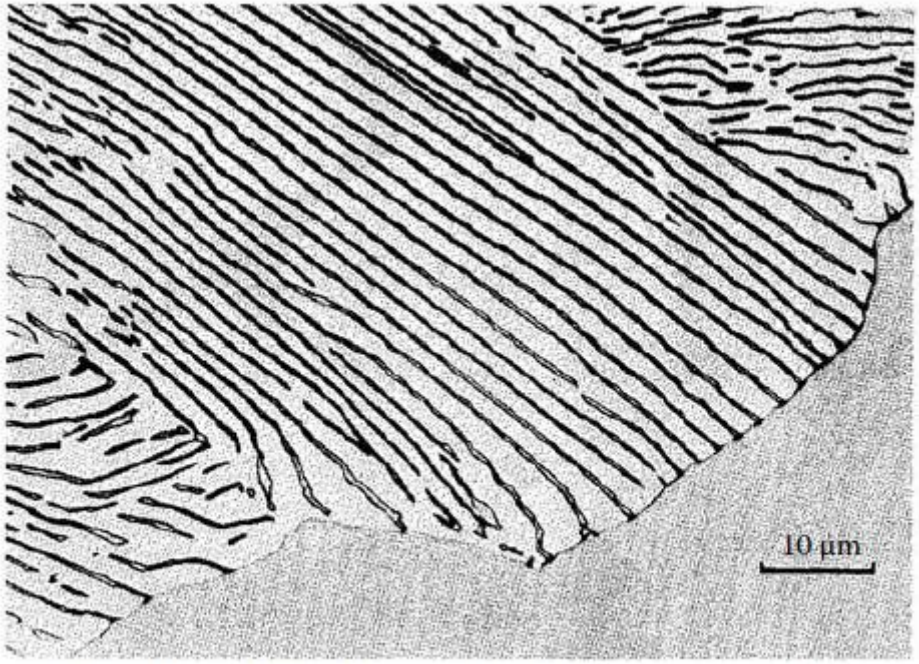

A pearlite colony advancing into an austenite grain.

At larger undercoolings the nucleation rate is much higher and *site saturation* occurs, that is all boundaries become quickly covered with nodules which grow together forming layers of pearlite outlining the prior austenite grain boundaries, Fig.

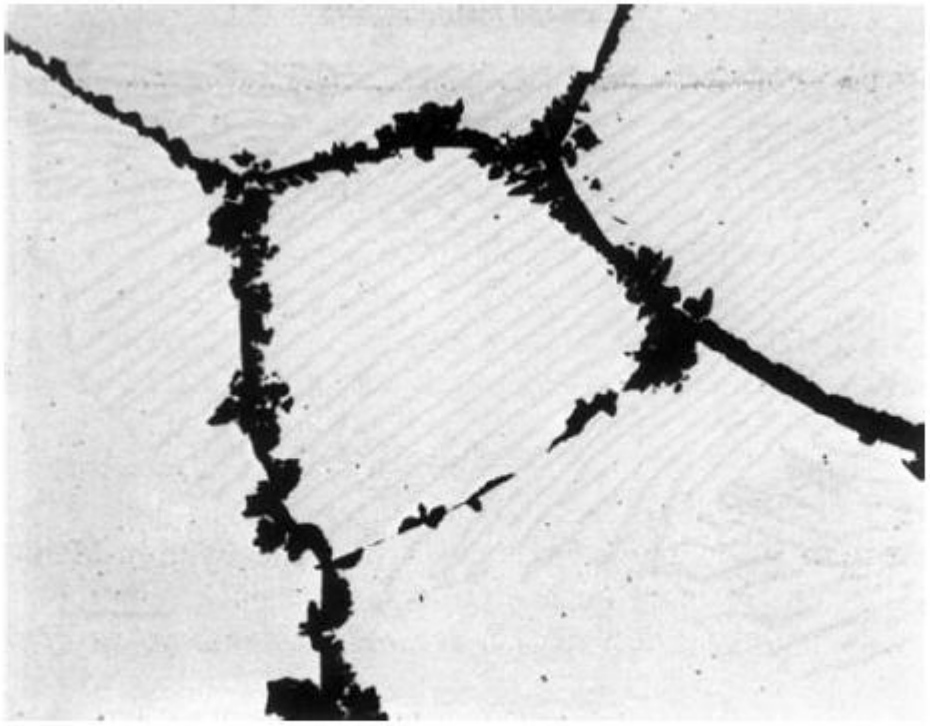

A partially transformed eutectoid steel. Pearlite has nucleated on grain boundaries and inclusions (× 100). (After J.W. Cahn and W.C. Hagel in *Decomposition of Austenite by Diffusional Processes,* V.F, Zackay and H.I. Aaronson (Eds.), 1962, by permission of The Metallurgical Society of AIME.)

Nucleation of Pearlite

The first stage in the formation of pearlite is the nucleation of either cementite or ferrite on an austenite grain boundary. Which phase nucleates first will depend on the grain-boundary structure and composition. Suppose that it is cementite. The cementite will try to minimize the activation energy barrier to nucleation by forming with an orientation relationship to one of the austenite grains, γ_1 in Fig-a. Therefore the nucleus will have a semicoherent, low mobility interface with γ_1 and an incoherent mobile interface with γ_2. The austenite surrounding this nucleus will become depleted of carbon which will increase the driving force for the precipitation of ferrite, and a ferrite nucleus forms adjacent to the cementite nucleus also with an orientation relationship to γ_1

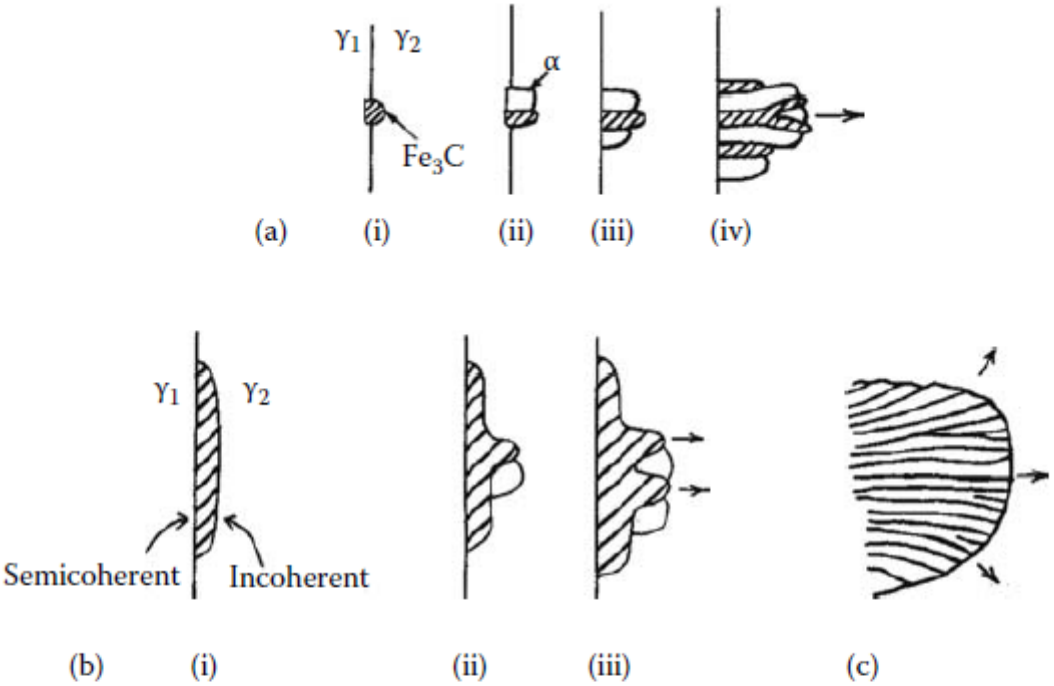

Nucleation and growth of pearlite. (a) On a "clean" grain boundary, (i) Cementite nucleates on grain boundary with coherent interface and orientation relationship with γ_1 and incoherent interface with γ_2 (ii) α nucleates adjacent to cementite also with a coherent interface and orientation relationship with γ_1 (This also produces an orientation relationship between the cementite and ferrite.) (iii) The nucleation process repeats sideways, while *incoherent* interfaces grow into γ_2 (iv) New plates can also form by a branching mechanism, (b) When a proeutectoid phase (cementite or ferrite) already exists on that boundary, pearlite will nucleate and grow on the incoherent side. A different orientation relationship between the cementite and ferrite results in this case, (c) A pearlite colony at a later stage of growth.

This process can be repeated causing the colony to spread sideways along the grain boundary. After nucleation of both phases the colony can grow edgewise by the movement of the *incoherent* interfaces, that is pearlite grows into the austenite grain with which it does not have an orientation relationship.

- If the alloy composition does not perfectly correspond to the eutectoid composition the grain boundaries may already be covered with a proeutectoid ferrite or cementite phase. If, for example, the grain boundary already contains a layer of cementite, the first ferrite nucleus will form with an orientation relationship to this cementite on the mobile incoherent side of the allotriomorphs as shown in Fig-b. Again due to the higher mobility of the incoherent interfaces the pearlite will grow into the austenite with which there is no orientation relationship.

Whatever the pearlite nucleation mechanism, new cementite lamellae are able to form by the branching of a single lamella into two new lamellae as shown in Fig-a(iv) or c. The resultant pearlite colony is effectively two interpenetrating single crystals.

It can be seen that the nucleation of pearlite requires the establishment of cooperative growth of the two phases. It takes time for this cooperation to be established and the rate of colony nucleation therefore increases with time.

Pearlite Growth

The growth of pearlite in binary Fe–C alloys is analogous to the growth of a lamellar eutectic with austenite replacing the liquid. Carbon can diffuse interstitially through the austenite to the tips of the advancing cementite lamellae so that the equations developed in Section «eutectic solidification» should apply equally well to pearlite. Consequently the minimum possible interlamellar spacing (S^*) should vary inversely with undercooling below the eutectoid temperature ($A_{1,\text{ eutectoid T}}$), and assuming the observed spacing (S_0) is proportional to S^* gives

$$S_0 \alpha\, S^* \alpha (\Delta T)^{-1}$$

Similarly the growth rate of pearlite colonies should be constant and given by a relationship of the type

$$v = kD_c^{\gamma}(\Delta T)^2$$

where k is a thermodynamic term which is roughly constant

In the case of binary Fe–C alloys, observed growth rates are found to agree rather well with the assumption that the growth velocity is controlled by the diffusion of carbon in the austenite. Figure shows measured and calculated growth rates as a function of temperature. The calculated line is based on an equation similar to equation ($v = kD_c^{\gamma}(\Delta T)^2$) and shows that the measured growth rates are reasonably consistent with volume-diffusion control.

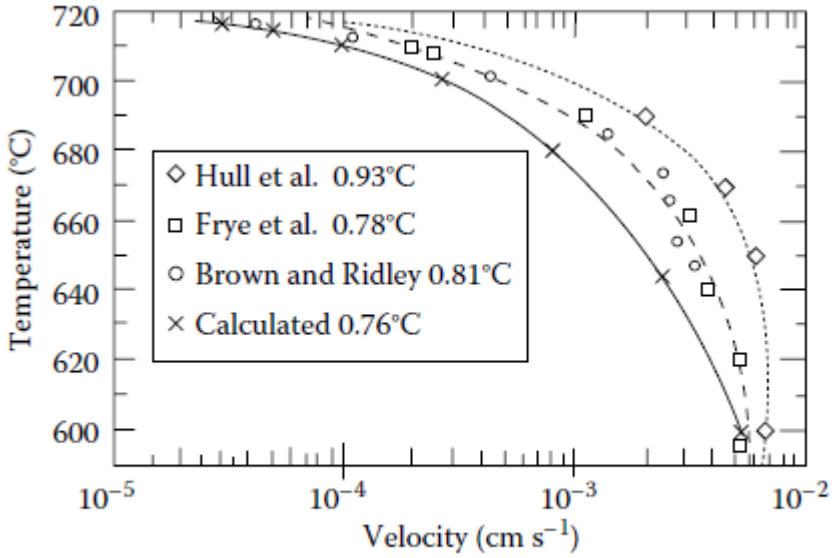

Pearlite growth rate v. temperature for plain carbon steels.

A schematic TTT diagram for the pearlite reaction in eutectoid Fe-C alloys is shown in Fig. Note the 'C shape typical of diffusional transformations that occur on cooling. The maximum rate of transformation occurs at about 550°C. At lower temperatures another type of transformation product, namely *Bainite,* can grow faster than pearlite. This transformation is dealt with in the next section.

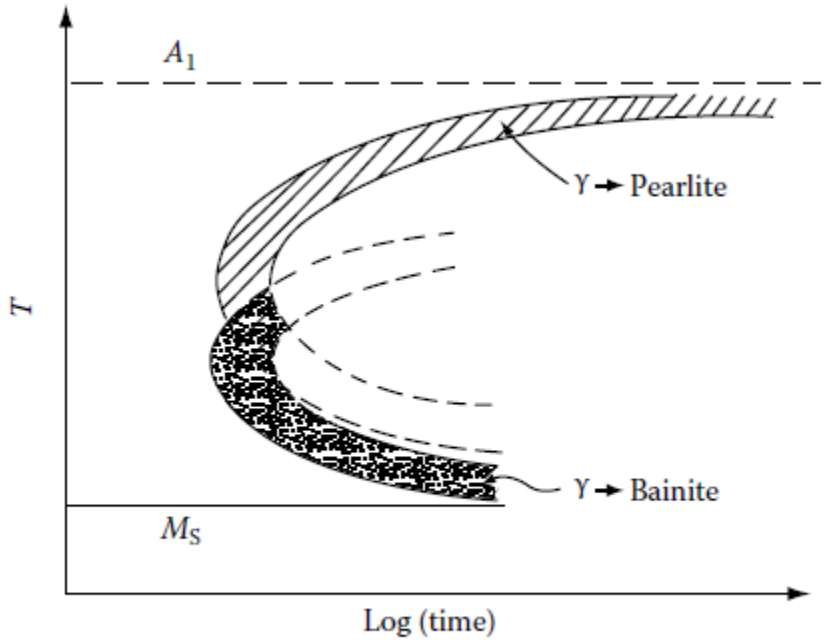

Schematic diagram showing relative positions of the transformation curves for pearlite and bainite in plain carbon eutectoid steels.

The Bainite Transformation

When austenite is cooled to large supersaturations below the nose of the pearlite transformation curve a new eutectoid product called *bainite* is produced. Like pearlite, bainite is a mixture of ferrite and carbide, but it is microstructurally quite distinct from pearlite and can be characterized by its own C curve on a TTT diagram. In plain carbon steels this curve overlaps with the pearlite curve so that at temperatures around 500°C both pearlite and bainite form competitively. In some alloy steels, however, the two curves are separated. The microstructure of bainite depends mainly on the temperature at which it forms.

Upper Bainite

At high temperatures (350°C–550°C) bainite consists of needles or laths of ferrite with cementite precipitates between the laths as shown in Fig. This is known as *upper bainite.* Fig-a shows the ferrite laths growing into partially transformed austenite. The light contrast is due to the cementite. Fig-b illustrates schematically how this microstructure is thought to develop. The ferrite laths grow into the austenite in a similar way to Widmanstatten side-plates.

- The ferrite nucleates on a grain boundary with a Kurdjumov-Sachs orientation relationship with one of the austenite grains, γ_2, say. Since the undercooling is very large the nucleus grows most rapidly into the γ_2 grain forming ferrite laths with low energy semicoherent interfaces. This takes place at several sites along the boundary so that a group of finely spaced laths develops. As the laths thicken the carbon content of the austenite increases and finally reaches such a level that cementite nucleates and grows.

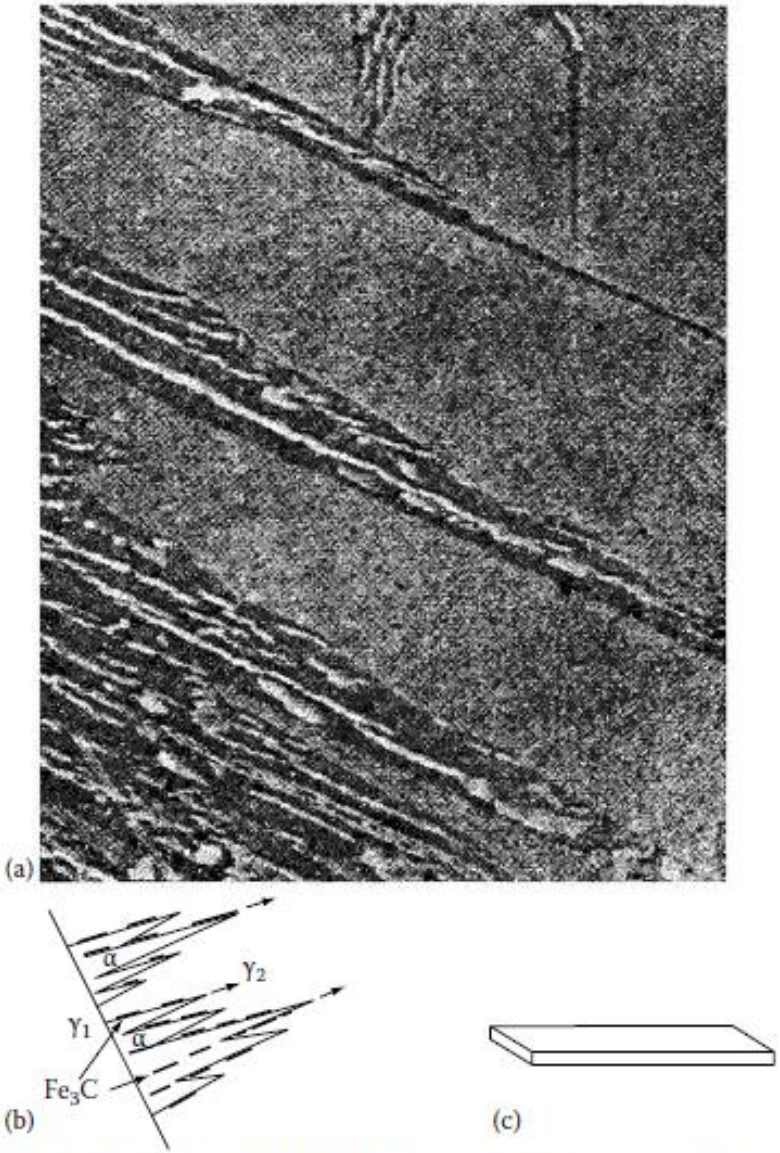

(a) Upper bainite in medium-carbon steel (replica × 13 000) (by permission of the Metals Society), (b) Schematic of growth mechanism. Widmanstatten ferrite laths growth into γ_2 (α and γ_2 have Kurdjumov–Sachs orientation relationship.) Cementite plates nucleate in carbon-enriched austenite. (c) Illustrating the shape of a 'lath'.

At the higher temperatures of formation upper bainite closely resembles finely spaced Widmanstatten side-plates. As the temperature decreases the bainitic laths become narrower so that individual laths may only be resolved by electron microscopy.

At the highest temperatures where pearlite and bainite grow competitively in the same specimen it can be difficult to distinguish the pearlite colonies from the upper bainite. Both appear as alternate layers of cementite in ferrite. The discontinuous nature of the bainitic carbides does not reveal the difference since pearlitic cementite can also appear as broken lamellae.
The greatest difference between the two constituents lies in their crystallography. In the case of pearlite the cementite and ferrite have ***no specific orientation*** relationship to the austenite grain in which they are growing, whereas the cementite and ferrite in bainite do have an ***orientation relationship*** with the grain in which they are growing.

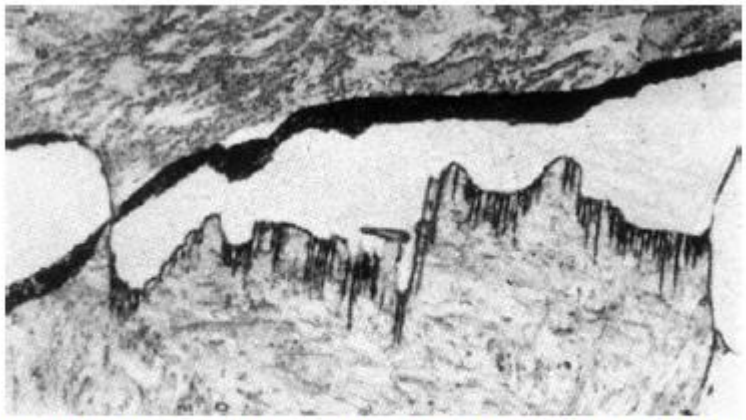

Hypoeutectoid steel (0.6% C) partially transformed for 30 min at 710°C, inefficiently quenched. Bainitic growth into lower grain of austenite and pearlitic growth into upper grain during quench (× 1800). (After M. Hillert in *Decomposition of Austenite by Diffusional Processes*, V.F. Zackay and H.I. Aaronson (Eds.), 1962, by permission of the Metallurgical Society of AIME.)

Lower Bainite

At sufficiently low temperatures the microstructure of bainite changes from laths into plates and the carbide dispersion becomes much finer. The temperature at which the transition to lower bainite occurs depends on the carbon content in a complex manner. For carbon levels below about 0.5 wt% the transition temperature increases with increasing carbon, from 0.5–0.7 wt% C it decreases and above approximately 0.7 wt% C it is constant at about 350°C.

At the temperatures where lower bainite forms the diffusion of carbon is slow, especially in the austenite and carbides precipitate in the ferrite with an orientation relationship. The carbides are aligned at approximately the same angle to the plane of the ferrite plate.

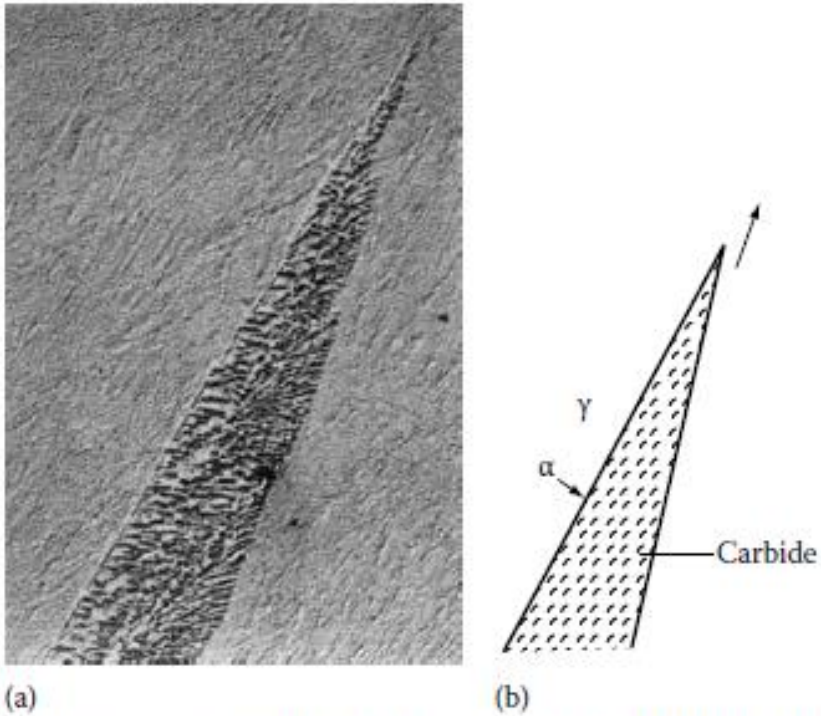

(a) (b)

(a) Lower bainite in 0.69wt% C low-alloy steel (replica × 1100). (After RF. Heheman in *Metals Handbook*, 8th edn., Vol. 8, American Society for Metals, 1973 p 196.) (b) A possible growth mechanism, α/β interface advances as fast as carbides precipitate at interface thereby removing the excess carbon in front of the α.